

**Measurement of ultralow interfacial tension with a laser interface manipulation technique**

Shujiro Mitani and Keiji Sakai

*Institute of Industrial Science, University of Tokyo, 4-6-1 Komaba, Meguro-ku, Tokyo 153-8505, Japan*

(Received 17 December 2001; revised manuscript received 10 April 2002; published 19 September 2002)

The liquid surface or interface is deformed slightly by a laser beam passing through it. Based on this principle, a method to measure the liquid-liquid interfacial tension is developed. The interfacial tension is determined from the deformation, of which the displacement is measured with another probe laser in a noncontact manner. The measurements were available in two different senses: the constant displacement under continuous laser irradiation gives the static value, and the frequency response spectrum of the displacement under modulated excitation gives the dynamic value. To demonstrate the usefulness of this method, a series of experiments were conducted in the interface between heptane and water containing aerosol OT as a surfactant. The interfacial tension was controlled by the concentration of added NaCl, and measurements were made over the range from 1  $\mu\text{N/m}$  to 100 mN/m of the tension. The results were in good agreement with the previous works. This method would be a new tool for the studies of various interfacial phenomena.

DOI: 10.1103/PhysRevE.66.031604

PACS number(s): 68.05.-n, 82.70.Uv, 78.20.-e

**I. INTRODUCTION**

Many experiments have been done recently on the mixtures of oil and water containing some surfactants. These systems have an interesting property: the interface between oil and water has very low tension less than 1 mN/m, which causes the appearance of various phases such as emulsion, microemulsion, or bicontinuous phase. They are quite important materials from a viewpoint of physical interest as well as industrial applications. For instance, studies have been done actively on the relation between the microstructure and the intermolecular force in microemulsions, and the developments of new medicines are made with emulsions. It is necessary, therefore, that the interfacial tension be measured precisely. Methods to measure the interfacial tension have already been established. One is Wilhelmy's hanging plate method. While this is a relatively easy technique, it is hard to measure low tensions because the tension is obtained by measuring the pulling force of the plate. In addition, the plate is in direct contact with the interface and may bring the interface some undesirable effect if the interface has some fragile structures such as an adsorbed molecular layer. Another one is the spinning-drop method: a thin tube containing water with an oil droplet is rotated and the change in the shape of the droplet gives the interfacial tension. Though useful for ultralow tension, the spinning-drop method is not effective for systems including a microemulsion [1,2].

We developed a noncontact interfacial tension meter useful over a wide range of tension, especially down to ultralow tension. Two focused laser beams are used in our method; one with a high intensity excites and deforms the interface [3] and the deformation is detected by the other one with a lower intensity. This technique can easily be understood in an analogy to the laser trapping technique, which is a noncontact manipulating tool of very small particles, so we call our method the laser interface manipulation technique (LIM). The LIM has three advantages over other measuring methods. First, the interfacial wave is generated by modulating the pump laser beam. The spectroscopy of the interfacial wave brings us various physical properties of the interface,

such as the dynamic interfacial tension and the interfacial elasticity. Secondly, the tension is obtained by measuring the interface deformation given by the external force. In Wilhelmy's method, for example, the tension is obtained as the force to pull down the plate. Hence, the lower the tension is, the less accurate the measurement is. In the LIM method, on the other hand, the deformation of the interface is larger when the tension is lower. The lower the tension is, the more accurate the measurement is. We can adjust the power of the pump laser beam to obtain a suitable displacement for measuring. The third advantage is the noncontact operation as mentioned above. In a contact method such as Wilhelmy's, it may happen that the interface is polluted by the probe contact. The contact method also induces a seriously large deformation of the interface, which might change the condition of the interfacial molecular layer.

The principle of the technique was already introduced in our previous work on liquid surfaces [4]. We measured the surface tension of a myristic acid monolayer with the laser-induced surface deformation technique (LISD). However, the surface tension was obtained as a relative value with respect to water and the accuracy was less than sufficient. The LISD technique has also been used in other works [5,6], in which the large deformations were excited in the liquid-liquid systems and the relation between the displacement of the interface and the pump laser intensity was studied. Their purpose was, however, to make the giant deformation, and not to study the interfacial properties. In this paper, we introduce a measurement system made to give the surface or interfacial tensions more accurately.

**II. DEFORMATION OF INTERFACE**

In our previous work, we discussed the surface properties of liquid under the approximation of high surface tension that simplifies the dispersion relation of the liquid surface wave. In a system with low tension, such as the liquid-liquid interface, this approximation loses validity. Hence, we rediscover the theory for the interface here.

The light propagates with the momentum, which is in-

versely proportional to the light wavelength in the medium. When the light travels from one medium with the index  $n_1$  and the density  $\rho_1$  to the other with  $n_2$  and  $\rho_2$ , discontinuity of the momentum at the interface applies the radiation pressure to the interface. Here, we adopt the condition  $\rho_1 > \rho_2$ ; this means that the light passes through the interface upward from the bottom. The equation of the momentum conservation is written with the radiation pressure  $p$ , which has a positive value in the upward direction:

$$\frac{n_1 i}{c} = (1-R) \frac{n_2 i}{c} - R \frac{n_1 i}{c} + p, \quad (1)$$

where  $i$  is the optical intensity per unit area and  $R$  is the energy reflectivity of the light given by  $R = (n_1 - n_2)^2 / (n_1 + n_2)^2$ . In the experiment, the light source is the laser beam and the intensity  $i$  has a spatial distribution given by

$$i(r) = \frac{2I_0}{\pi w^2} \exp\left(-\frac{2r^2}{w^2}\right), \quad (2)$$

where  $I_0$  is the total light intensity,  $r$  is the distance from the beam center, and  $w$  is the width of the laser beam. Then, the radiation pressure at the position  $r$  is written as

$$p(r) = -\frac{2I_0}{c\pi w^2} (n_2 - n_1) \left(1 - \frac{n_2 - n_1}{n_2 + n_1}\right) \exp\left(-\frac{2r^2}{w^2}\right). \quad (3)$$

According to Eq. (3), the radiation pressure works to push the interface into the material with a smaller refractive index regardless of the propagation direction. At the interface, this force is balanced with gravity and the Laplace force. The interface displacement  $\xi(r)$  is given by

$$p(r) - \Delta\rho g \xi(r) + \gamma \nabla^2 \xi(r) = 0, \quad (4)$$

where  $\xi$  has a positive value in the vertical upside,  $\Delta\rho$  represents the difference in density as  $\Delta\rho = |\rho_1 - \rho_2|$ ,  $g$  is the gravity constant, and  $\gamma$  is the interfacial tension. From Eqs. (3) and (4), the displacement of the interface is represented as

$$\xi(r) = \frac{w^2 P_0}{4} \int_0^\infty \frac{k J_0(kr) \exp(-w^2 k^2 / 8)}{\gamma k^2 + \Delta\rho g} dk. \quad (5)$$

Here,  $J_0$  is the zeroth-order Bessel function and  $P_0$  is given by

$$P_0 = -\frac{2I_0}{c\pi w^2} (n_2 - n_1) \left(1 - \frac{n_2 - n_1}{n_2 + n_1}\right). \quad (6)$$

Figure 1 shows the curves of  $\xi(r)$  calculated for the different values of  $\gamma$ . As is easily understood with the principle of the optical deformation, the interface in the radiated area,  $r < w$ , is convex, while the outer area is concave showing the meniscus to the flat interface. The measurement of  $\xi(r)$  brings us the interfacial tension with two possible approaches: (a) the static measurement and (b) the spectroscopic one.

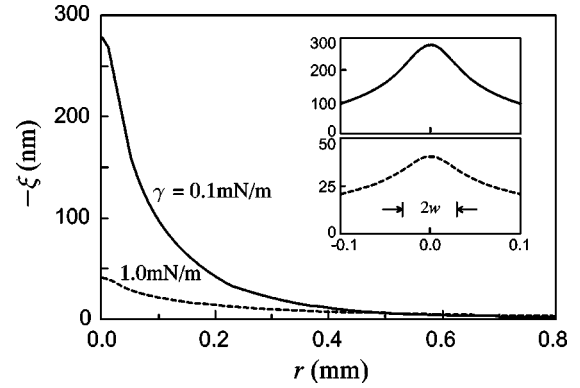


FIG. 1. Calculated curves of interface displacement under pump laser with  $\lambda = 532$  nm,  $w = 30$   $\mu\text{m}$ , and  $I_0 = 400$  mW. The liquids are of  $n_1 = 1.332$ ,  $n_2 = 1.385$ , and  $\Delta\rho = 0.32$  g/cm<sup>3</sup>. The insets represent the shape around the center of the deformation in an expanded axis.

### A. Static measurement of interface deformation

The deformed shape of the interface is uniquely determined by Eq. (5) together with the material properties and the optical conditions. Here, we assume that all of these parameters are given and kept constant except the interfacial tension, and the interface deformation is thus a unique function of  $\gamma$ . We can, therefore, determine the interfacial tension by measuring only one characteristic value of the deformed interface, such as (i) the absolute value of the peak height  $\xi(0)$ , (ii) the curvature of the interface at the center  $\partial^2 \xi(0) / \partial r^2$ , or (iii) the maximum gradient of the deformed interface which appears at around  $r = w$ , as shown in Fig. 1. We have actually tried to measure these values. Each of them is shown to have both advantages and disadvantages.

While the absolute peak height can be accurately measured by the optical interference, the signal is very sensitive to the mechanical noise of vibration. In addition, the method is complicated when the displacement exceeds half of the optical wavelength, as in the present case. As for the measurement of the interface curvature, which we actually adopted in our previous work, the detected signal is easily analyzable in terms of the simple expression of the coaxial optics of the pump and probe laser beams. However, we have to carry out some complicated calculations to relate the detected signal to the absolute value of the interface curvature. The coaxial configuration has some experimental problems when applied to the light absorbable materials. The probe laser passed the same way, as the pump suffers from a serious thermal lens effect.

The interface gradient is, within the first approximation, the most intuitive measure obtained by the optical technique since the deflection angle of the reflected light directly gives twice the surface gradient. Therefore, we tried this method in the present experiment, though other methods are also useful for different conditions.

Of course, we have to accurately calculate the beam deflection and distortion after the penetration of the deformed interface since the probe and pump laser have finite and comparable beam size. The calculation of the far-field profile of the probe laser was carried out as follows: The probe laser is

an ideal Gaussian beam convergent almost normally to the interface where the beam has its waist. While the flat interface works as a flat mirror, the interface suffering from the deformation modulates the phase of the incident probe beam. We consider approximately that the probe laser is normally incident to the interface and suffers from the phase shift  $\phi(\mathbf{r})$  dependent on the position on the interface  $\mathbf{r}$  and related to the interface displacement  $\xi(\mathbf{r})$  to  $\phi(\mathbf{r})=2k_{\text{pr}}\xi(\mathbf{r})$ ,  $k_{\text{pr}}$  being the wave number of the probe laser in the medium 1. The far-field pattern of the probe laser beam after reflection is given by the Fourier transformation of the modulated beam pattern as

$$I'_{\text{pr}}(\mathbf{r}') = \int I_{\text{pr}}(\mathbf{r}) \exp\{i\phi(\mathbf{r})\} \exp(i\mathbf{K}\mathbf{r}') d\mathbf{r}, \quad (7)$$

where  $I_{\text{pr}}$  is the incident probe profile and  $\mathbf{K} = (k_{\text{pr}} \sin \theta \cos \varphi, k_{\text{pr}} \sin \theta \sin \varphi)$ ,  $\theta$  is the deflection angle taken from the normal, and  $\varphi$  is the azimuth angle. The change in the beam profile is calculated with the actual experimental conditions and shown later in Sec. III. In the experiment, we do not have to observe the whole shape of the far-field pattern but measure a portion of the pattern at an appropriate fixed point. The above calculation gives all the information to relate the optical power cut by a pinhole to the absolute interface displacement and thus the interfacial tension.

### B. Response spectroscopy of the interface

By modulating the intensity of the pump light, the interface is oscillated and the interfacial wave is excited and propagates. The response of the interface to the pump light brings us the dynamic interfacial tension of the materials. Measuring the frequency response spectrum of the interface is quite important in the LIM method. In this technique, the time-dependent displacement of the interface is given as the summation of the propagating or damping waves with different wave numbers. When the pump laser intensity is modulated with the frequency  $\omega$ , the interface displacement is represented as [4]

$$\xi(r, t) = \frac{w^2 P_0}{4} \int_0^\infty \frac{k^2 J_0(kr)}{\omega^{*2} - \omega^2} \exp\left(\frac{-w^2 k^2}{8}\right) \exp(i\omega t) dk. \quad (8)$$

Here,  $k$  is the wave number of the propagating wave. The complex angular frequency  $\omega^*$ , whose real and imaginary parts represent the frequency and damping constant, respectively, has the relation with  $k$  given by

$$\left(i\omega^* + 2\frac{\eta}{\rho}k^2\right)^2 + \frac{\gamma}{\rho}k^3 + \frac{\Delta\rho}{\rho}gk = 4\frac{\eta^2}{\rho^2}k^4 \left(1 + \frac{i\rho\omega^*}{\eta k^2}\right)^{1/2}, \quad (9)$$

where  $\eta = \eta_1 + \eta_2$  is the total viscosity of the two materials, and  $\rho = \rho_1 + \rho_2$  is the total density [7].

As shown in Fig. 1, the deformed interface has a convex peak in the laser-illuminating region with a broad skirt of the

meniscus. The typical and finest structure of the deformation is thus restricted by the pump beam width. The wave number of the excited interfacial wave under the periodic modulation of the pump laser power is also restricted to about  $k \sim \pi/2w$ , which gives the characteristic form of the frequency spectrum of the interface deformation. The amplitude of the interface vibration decreases rapidly at around the characteristic frequency  $f_c$ , which is roughly estimated to  $2\pi f_c \sim (\gamma/\rho)^{1/2}(\pi/2w)^{3/2}$ . The observation of the characteristic frequency then leads to the absolute value of the interfacial tension. This is the principle of the dynamic measurement.

In the experiment of the dynamic measurement, we do not have to obtain the absolute value of the interface displacement, but only to get the frequency spectrum of the dynamic deformation. Therefore, we measured the interface gradient instead of the absolute displacement by the same method described above. The signal is proportional to the inclination of the interface at  $r=w$ , which is given by

$$S(\omega) \propto \int_0^\infty \frac{k^3 J_1(kw) \exp(-k^2 w^2/8)}{\omega^2 - \omega^{*2}} dk. \quad (10)$$

To be precise, the term of the phase retardation due to the wave propagation in the distance  $w$  is neglected. Equation (10) approximately gives the correct spectrum, as long as we note only the amplitude of the signal in the present case. At the low-frequency limit,  $S(\omega)$  gives the static value  $S_0$  leading to the actual displacement  $\xi(0)$ . The signal decreases with increasing frequency at around  $\omega \sim |\omega^*|$ . We redefine here the characteristic frequency  $\omega_c$  as that gives a half-signal intensity of  $S_0$  and  $S(\omega_c) = S_0/2$  for the further discussion.

Here, we have to pay attention to the fact that the interfacial tension of the present experiment ranges widely from  $10^{-1}$  to  $10^{-6}$  N/m. The typical characteristic frequency  $\omega_c$  of the interface motion is determined by the condition that the sum of the inertia and the viscous force is balanced to the capillary force of the curved interface. By assuming that the interface region of  $w \times w$  has the displacement  $\xi$  and the stress reaches the depth of  $w$ , the inertia and viscous force are roughly estimated to be  $\rho w^2 \xi/T^2$  and  $\eta w \xi/T$ , respectively,  $T$  being the characteristic time constant of the motion. By comparing them to the capillary force  $\gamma \xi$ , we can know which factor plays the major role in the interface motion. As for the water surface, for example with  $\gamma = 0.07$  N/m,  $w = 10^{-4}$  m,  $\rho = 10^3$  kg/m<sup>3</sup>, and  $\eta = 10^{-3}$  Ns/m<sup>2</sup>, the typical time constant required to be equal to the capillary force is  $T = 0.12$  ms for inertia and  $T = 1.4$   $\mu$ ms for the viscous term. This means that the inertia is dominant. On the other hand, as for the surface of  $\gamma = 1$   $\mu$ N/m, the time constants are 30 and 100 ms for the inertia and viscous term, respectively. These two factors are comparable and the approximate expression of the dispersion relation used in Ref. [7] is no longer correct. We therefore employed the strict form of the dispersion equation representing the relation between the complex eigenfrequency and the wave number as Eq. (9).

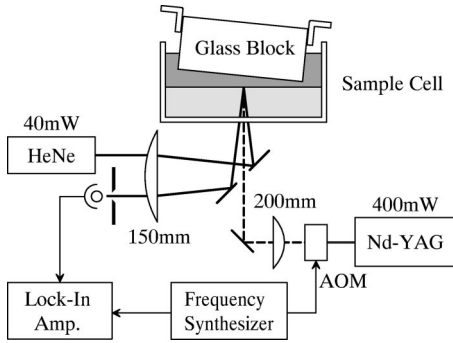


FIG. 2. Experimental setup of the LIM technique. The pump laser beam has  $I_0 = 190$  mW at the interface.

III. EXPERIMENTAL SETUP

Though the basic concept is the same as our previous study [4], the target in this study is on the interface of two liquids and there are some improvements in the present measurement system. The experimental setup is schematically shown in Fig. 2. Deformation of the interface is excited by a frequency-doubled cw-Nd:YAG laser with maximum output power 400 mW and wavelength 532 nm. The beam diameter at the output is 2.2 mm. The pump laser beam is focused onto the liquid interface by a lens with the focal length 200 mm upward through the bottom of the sample cell. The focused diameter of the pump laser beam is 62  $\mu\text{m}$ . The reason for irradiating from the backside is that the thermal expansion of water by pump laser is only 1/5 that of oil and may do less harm to the undesirable thermal deformation.

To detect the displacement of the excited interface, we used a He-Ne laser with output power 40 mW and 1.7 mm beam diameter as a probe. The probe light is focused by a lens with the focal length 150 mm to a spot with 71  $\mu\text{m}$  diameter on the excited area of the interface near the pump light, and reflected to the detector. To measure the maximum interface gradient, the position of the probe light giving the maximum signal is found by sweeping the probe laser. The deformed interface works as a curved mirror. When the pump light is on and the interface is deformed, the reflected probe light goes to a different direction. We switched on and off the YAG laser with the acousto-optic modulator (AOM) and detected the intensity of the reflected probe light through a pinhole with 100  $\mu\text{m}$  diameter. In this experiment, the observation distance was the length between the lens and the interface, which is equal to the focal length and 150 mm. The signal is detected by a lock-in amplifier to which the reference is given by the modulation signal. To avoid a troublesome reflection at the air-oil interface on the top, we placed a glass block above the interface so that the bottom face made a slight tilt to the horizon. This glass block has another effect to stabilize the interface; without it, the liquid-liquid interface may sway, influenced by the air-oil vibration.

In this work, we used the sample cell with an optically flat glass window that is commercially available. An important point required of the sample cell is that the pump and probe laser beam arrive at the interface of liquid without any distortion of the beam profile. This modest requirement of the

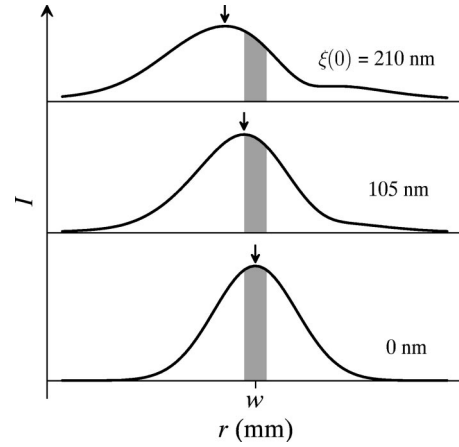


FIG. 3. Intensity profiles of a reflected probe laser beam for different values of  $\xi(0)$ . The grayed area shows the position detected through the pinhole.

sample container would be advantageous in industrial applications.

Under the experimental conditions described above, we calculated the beam profile of the probe laser light after reflection and distortion by the deformed interface with Eq. (7), which is shown in Fig. 3. Here, we assumed that the power of the pump laser is kept constant,  $I_0 = 190$  mW, and the interfacial tension is swept to bring about the change in the absolute peak height  $\xi(0)$ . We can see the distortion of the beam profile from the Gaussian, as well as the shift in the peak position. The peak shift at  $\xi(0) = 210$  nm is about 0.36 mm, which is in the same order of the rough estimation of the interface gradient  $\Delta \sim \xi(0)/w \sim 6 \times 10^{-3}$  rad and the focal length  $L = 150$  mm to  $\delta \sim 2L\Delta \sim 1.0$  mm. The discrepancy is probably due to the fact that the interface is concave at  $r = w$  and the reflection is suppressed.

In the experiments, we set a pinhole to pick up the portion of the reflected light to convert the distortion of the beam profile to the change in the optical intensity. The optical intensity  $I_{pr}$  picked up by a pinhole is represented as shadows in Fig. 3. Figure 4 shows the theoretical curve to relate  $\xi(0)$  to the change in the optical intensity  $(I_{flat} - I_{pr})/I_{flat}$ ,  $I_{flat}$  being the intensity without the optical deformation and  $\xi(0) = 0$ . Since the excess deformation may lead to signal saturation, as shown in Fig. 4, we adjusted the pump laser intensity

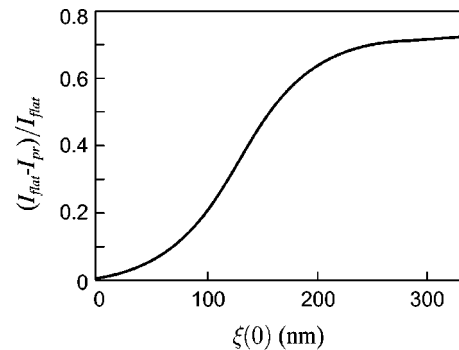


FIG. 4. The relation between  $\xi(0)$  and  $(I_{flat} - I_{pr})/I_{flat}$  corresponding to the pump laser shown in Fig. 1.

with an ND filter to keep  $I_{pr}/I_{flat}$  at an optimum range in which the relation between  $\xi(0)$  and  $(I_{flat} - I_{pr})/I_{flat}$  has linearity.

To summarize the procedure of the analysis, we first calculate the interface deformation at each interfacial tension with known optical conditions. The far-field pattern is then given numerically through Eq. (7), which is finally related to the signal intensity.

In the measurement of the dynamic response of the interface under the periodical modulation by the pump laser intensity, we do not require absolute information on the interface deformation but the characteristic frequency where the signal decreases to 1/2 of the static value.

#### IV. RESULTS AND DISCUSSIONS

To confirm the validity of the LIM method in measuring the interfacial tensions, we made the experiments with the actual sample of a free surface of oil and an oil/water interface. The materials were 1-Octanol as the oil and distilled water. The refractive indexes and the densities of the sample liquids were measured by the Abbe refractometer and the density meter, respectively.

First, we carried out the static experiment of the surface tension of Octanol by measuring the absolute value of  $(I_{flat} - I_{pr})/I_{flat}$ . The result for the air/Octanol interface is 24.5 mN/m at 27°C while the value is 26.9 mN/m in the previous work [8]. This shows that the LIM method is useful for the measurement of the surface tension even in the region over 10 mN/m. The reason for a slight disagreement between the present and the previous work is that in the LIM method the surface with large tension is difficult to deform by the pump light and the error in the observed displacement may increase. We also carried out the dynamic measurement for the same surface and obtained the dynamic surface tension to 25.6 mN/m by fitting the theoretical spectrum of Eq. (10) to the experimental result. As for the difference between the static and the dynamic values, the experimental error is attributed to the static measurement that is subject to the mechanical vibration. Both experiments are carried out also for the liquid/liquid interface of the water/Octanol system. The result is 8.55 mN/m (static) and 8.62 mN/m (dynamic) at 25°C, which agreed well with the value 8.4 mN/m in the other work [9]. These results show that the interfacial tensions, not only the surface, can be measured precisely with our method.

To apply the LIM method to observe the interfacial properties, we made a series of experiments for the interface in which the tension changes with the ion concentrations. The ionic surfactant, AOT for instance, changes its affinity to water or to oil depending on the concentration of salt. Therefore, the interfacial tension in the system of oil and water with an ionic surfactant often makes a drastic change with a minimum value [10]. The range of the tension is lowered from 1 mN/m to 1  $\mu$ N/m. In the previous works, the experiments have been made with the spinning-drop and the light scattering method, which are good to measure the low interfacial tensions but have some difficulty in the operation. We made a series of experiments and obtained  $\gamma$  in the systems

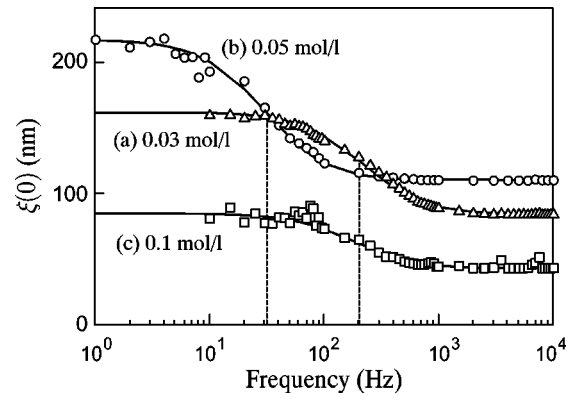


FIG. 5. Typical examples of the spectra obtained in the heptane-water-AOT systems with NaCl concentration of (a) 0.03 mol/l, (b) 0.05 mol/l, and (c) 0.1 mol/l. The dashed lines represent the cutoff frequencies which coincide between (a) and (c).

of heptane, water, and sodium di(2-ethylhexyl) sulfosuccinate, generally referred to as aerosol OT, with different concentrated NaCl of 0.01–0.1 %, which is the same condition as in Ref. [10]. The concentration of AOT to water was  $2.47 \times 10^{-3}$  mol/l, which is a little lower than the CMC of AOT of  $2.5 \times 10^{-3}$  mol/l, and there were no micelle in pure water. This interface is known to show drastic change in the interfacial tension with a small amount of added NaCl. In our method, the interface is required to be flat as a mirror, so the water with AOT and NaCl was first poured into the sample cell, and then heptane was poured onto the water gently. We began the measurement 5 h after the sample preparation. In the appearance of the microemulsion in the 0.05 mol/l NaCl system, the reflected probe light was partly scattered and weakened. While the static measurement lost accuracy in such a situation, the response spectrum of the interface was obtained without any serious problems.

Figure 5 shows typical examples of the frequency response spectra of the interface in systems with different salt concentrations. The vertical axis is normalized so that the low-frequency limits of the dynamic response signal agree with the absolute values of the interface deformation  $\xi(0)$  measured by the static measurement. The solid lines are the spectra of Eq. (10) fitted with  $\gamma$  as the running parameter. As shown in the figure, the amplitude gradually decreases as frequency increases, suggesting that the interface is reluctant to quick motions and that the wave would have an upper limit in the wave number. Experimental points are in good agreement with the theoretical curves, and the cutoff frequency corresponding to the limiting wave number is shown with dashed lines. As shown in the figure, the cutoff frequency and the limiting amplitude at lower frequency depend on the salt concentration. The spectrum (b) has the lowest cutoff frequency of the three:  $\omega_c \sim 30$  Hz in (b), while  $\omega_c \sim 200$  Hz in (a) and (c). This means, as mentioned in Sec. II, that the interfacial tension of (b) is the lowest of the three. The largest amplitude of (b) also supports this fact. It seems that the interfacial tension of (a) is nearly equal to that of (c) in spite of the difference in the NaCl concentration.

The static and dynamic interfacial tensions obtained from

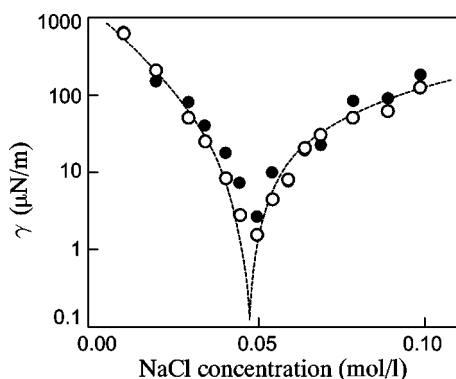


FIG. 6. Observed interfacial tension vs the salt concentrations. The open and closed circles represent the dynamic and the static tensions, respectively. The dashed line shows the result of the previous work by Aveyard *et al.*

the spectra are shown in Fig. 6. In this figure, the dashed line represents the previous result obtained with the spinning drop method [10]. Both the static and dynamic results are in good agreement with the previous work. It is also found that the interfacial tension depends on the concentration of NaCl and has a minimum at about 0.05 mol/l. In the oil-water-surfactant system, the interfacial tension between oil and water is determined by the ionization of AOT. In the low salt concentration, AOT is easily ionized because of the absence of the counterion, and AOT is highly hydrophilic and less effective as a surfactant:  $\gamma$  is high. As the salt concentration

increases, the ionization of AOT decreases gradually because ionization is suppressed by the counterions of  $\text{Na}^+$ . At the salt concentration of 0.05 mol/l, the balance between the hydrophilic and hydrophobic nature gives the lowest interfacial tension. With more salt, the nonionized AOT molecules increase and the AOT becomes too hydrophobic and  $\gamma$  is high.

In conclusion, we summarize the advantages of this laser-interface manipulation method as a new technique for measuring the interfacial tension. It is useful over a wide dynamic range from  $10^2$  mN/m down to  $10^{-3}$  mN/m providing us with a sufficient accuracy up to  $\pm 0.2\%$ . The key point is in the laser manipulation: We can adjust the driving power depending on the interfacial tension of the specimen under study, and make the ideal deformation for accurate measurement. Further, the simple handling and the noncontact operation of this system have a great advantage in the measurements of very delicate interfaces appearing, for instance, in the critical consolute phenomenon, or fluids in the medical production lines that strongly resist being contaminated. This technique has the potential to meet the demands of fundamental scientific studies, as well as industrial evaluation technology.

#### ACKNOWLEDGMENT

This work was partially supported by a Grant-in-Aid for scientific research from the Ministry of Education, Science, Sports and Culture.

- 
- [1] R.J. Good, J.T. Ho, G.E. Broers, and X. Yang, *J. Colloid Interface Sci.* **107**, 290 (1985).  
 [2] R.J. Good, C.J. Vanoss, G.E. Broers, and Y. Xin, *J. Colloid Interface Sci.* **110**, 604 (1986).  
 [3] A. Ashkin and J.M. Dziedzic, *Phys. Rev. Lett.* **30**, 139 (1973).  
 [4] K. Sakai, D. Mizuno, and K. Takagi, *Phys. Rev. E* **63**, 046302 (2001).  
 [5] A. Casner and J.P. Delville, *Phys. Rev. Lett.* **87**, 054503 (2001).  
 [6] A. Casner and J.P. Delville, *Opt. Lett.* **26**, 1418 (2001).  
 [7] V.C. Levich, *Physicochemical Hydrodynamics* (Prentice-Hall, Englewood Cliffs, NJ, 1962).  
 [8] J.J. Jasper, *J. Phys. Chem. Ref. Data* **1**, 841 (1972).  
 [9] R. Steinberger, *Kolloid Z. Z. Polym.* **195**, 8 (1964).  
 [10] R. Aveyard, B.P. Binks, T.A. Lawless, and J. Mead, *Can. J. Chem.* **66**, 3031 (1988).